coatings

MDPI

Article

Fluorination of TiN, TiO_2, and SiO_2 Surfaces by HF toward Selective Atomic Layer Etching (ALE)

Ju Hyeon Jung, Hongjun Oh and Bonggeun Shong *

Department of Chemical Engineering, Hongik University, Seoul 04066, Republic of Korea
* Correspondence: bshong@hongik.ac.kr

Abstract: As semiconductor devices become miniaturized, the importance of the molecular-level understanding of the fabrication processes is growing. Titanium nitride (TiN) is an important material utilized in various architectural components of semiconductor devices requiring precise control over size and shape. A reported process for atomic layer etching (ALE) of TiN involves surface oxidation into titanium oxide (TiO_2) and selective oxidized layer removal by hydrogen fluoride (HF). However, the chemical selectivity of these Ti-based materials in the etching process by HF remains unclear. In this study, computational chemistry methods utilizing density functional theory (DFT) calculations were applied to the fluorination reactions of TiN, TiO_2, and SiO_2 to identify and compare the surface chemical reactivity of these substrates toward etching processes. It is shown that the materials can be etched using HF, leaving TiF_4 and SiF_4 as the byproducts. However, while such a TiN reaction is thermodynamically hindered, the etching of TiO_2 and SiO_2 is suggested to be favorable. Our study provides theoretical insights into the fluorination reactivity of TiN, which has not been reported previously regardless of technological importance. Furthermore, we explore the etching selectivity between TiN, TiO_2, and SiO_2, which is a crucial factor in the ALE process conditions of TiN.

Keywords: fluorination; etching; titanium nitride; titanium dioxide; silicon dioxide; computational chemistry

Citation: Jung, J.H.; Oh, H.; Shong, B. Fluorination of TiN, TiO_2, and SiO_2 Surfaces by HF toward Selective Atomic Layer Etching (ALE). *Coatings* **2023**, *13*, 387. https://doi.org/10.3390/coatings13020387

Academic Editors: Ivan A. Pelevin and Dmitriy Yu. Ozherelkov

Received: 15 January 2023
Revised: 5 February 2023
Accepted: 7 February 2023
Published: 8 February 2023

1. Introduction

Titanium nitride (TiN) is an important industrial material with various widespread applications because of its excellent mechanical stability and good electrical and thermal conductivity. In the semiconductor industry, it is used as a diffusion barrier between interconnect metals such as copper (Cu) with dielectric layers. In addition, it is employed as metal gate electrodes due to its chemical stability and good adhesion to the substrates [1–5]. TiN is also highly resistant to corrosion and can withstand high temperatures, making it suitable for use in the aerospace and automotive industries, such as in wear-resistant coating and other high-stress applications [6–8]. Despite the excellent chemical resistance of the bulk TiN material, its surface can be oxidized under exposure to an oxidative atmosphere [9].

Atomic layer etching (ALE) is a technique used in microfabrication and nanofabrication to precisely etch thin layers of material from a substrate [10–14]. One of the key advantages of ALE over other etching techniques is its ability to achieve high precision levels and control over the etch depth. The thickness of the material removed in each cycle of the ideal ALE process is a constant value, thus the etched material's total thickness can be precisely controlled by adjusting the number of ALE cycles performed. In addition, the highly conformal nature of ALE makes it possible to etch inside features with high aspect ratios [15]. ALE involves sequential substrate exposure to a series of gases, reacting with the surface to remove a material layer [16]. Such a process mainly consists of two chemical reactions. First, a converted layer is formed by the reaction between the first etchant and

the substrate. As the reaction between the second etchant and the converted layer proceeds, volatile byproducts are generated, thereby etching the surface.

The ALE process of TiN has been developed following the miniaturization of semiconductor devices. In a reported ALE process of TiN [17], the first conversion reaction forms a TiO_2 layer using oxidizing agents such as O_3 or H_2O_2, whose thickness is quasi-limited by slow O diffusion into TiO_2. Then, hydrogen fluoride (HF) etchant reacts with TiO_2 in the second reaction to produce the volatile byproducts H_2O and TiF_4. However, because HF does not etch TiN, the etch process effectively stops when TiO_2 is completely removed and TiN becomes exposed. Therefore, a constant etching rate, often called etch per cycle (EPC), can be achieved, which is a requirement for ALE. In other words, the difference in etching tendency between TiN and TiO_2 by HF plays a decisive role in the ALE process of TiN. A few other alternatives that reported the ALE processes of TiN also involve the liberation of Ti via halogenation either by F or Cl [18–20]. In addition, SiO_2 is ubiquitously used in the semiconductor industry, which is known to be etched through a fluorination reaction with HF [21,22]. However, in the aforementioned report on thermal ALE of TiN, an optimized TiN ALE process showed high selectivity against SiO_2, so that the etching rate was significantly higher for TiN than SiO_2 [17].

Using atomistic computational chemistry simulations, the pathways of each reaction in the etching processes can be explored, and volatile byproducts can be inferred [23,24]. However, since the thermal ALE processes present various theoretical challenges, such as self-limiting reactions and the generation of volatile reaction products, only limited studies have been conducted to identify the reaction mechanisms [25–32]. In particular, while the process conditions for fluorination and removal of Ti atoms from TiO_2 by HF were previously molecularly elucidated [33,34], its selectivity against TiN or SiO_2 substrates is yet to be known.

In this study, the reactivity toward the etching of TiN, TiO_2, and SiO_2 substrates by HF is comparatively investigated using density functional theory (DFT) calculations. The molecular adsorption mechanism of HF and possible etching products, such as TiF_4, NH_3, H_2O, and SiF_4, were identified. It was observed that the dissociative HF adsorption and the subsequent TiF_4 desorption are preferable on TiO_2 but not on TiN. The etching of SiO_2 by HF was also found to be possible.

2. Computational Methods

DFT calculations were performed using the Vienna ab initio simulation package version 5.4.4. The PBE exchange-correlation functional and D3BJ dispersion correction were applied with projector-augmented wave methods. Surface models of rocksalt cubic TiN (001), anatase TiO_2 (101), and quartz SiO_2 (0001), which are known to be the most stable crystalline orientations of each material, were constructed (Figure 1). The top layers close to the surface were optimized, while the bottom layers were fixed at their ideal crystalline positions. Cut-off energy values of (450, 450, 500 eV), and slab sizes in (length × width × height) of (4.21 × 4.21 × 10.94), (10.46 × 7.61 × 10.30), and (4.93 × 4.93 × 11.86) $Å^3$ were used for TiN, TiO_2, and SiO_2, respectively. The vacuum space between the slabs was 15 Å to prevent unphysical interlayer interactions. All calculations applied Monkhorst-Pack k-point mesh settings of 5 × 5 × 1.

Calculations were performed to compare the reaction pathways and energies of HF for the three substrates. For the TiN and the SiO_2 substrates, 1 to 4 HF molecules were added. In the case of the TiO_2 substrate with a larger size, the calculation was performed by adding 4, 8, 12, and 16 HF, respectively, according to the size ratio. Each energy was divided by the number of HF to confirm the reaction tendency for each substrate.

The electronic energies of adsorption and desorption reactions (E_{ads}) are expressed by the following equation:

$$\begin{aligned} E_{ads} &= \left(E_{adsorption} + E_{byproduct}\right) - \left(E_{slab} + E_{HF}\right) \\ \text{Here, } E_{ads} &= \left(E_{adsorption} + E_{byproduct}\right) - \left(E_{slab} + E_{precursor}\right) \end{aligned} \quad (1)$$

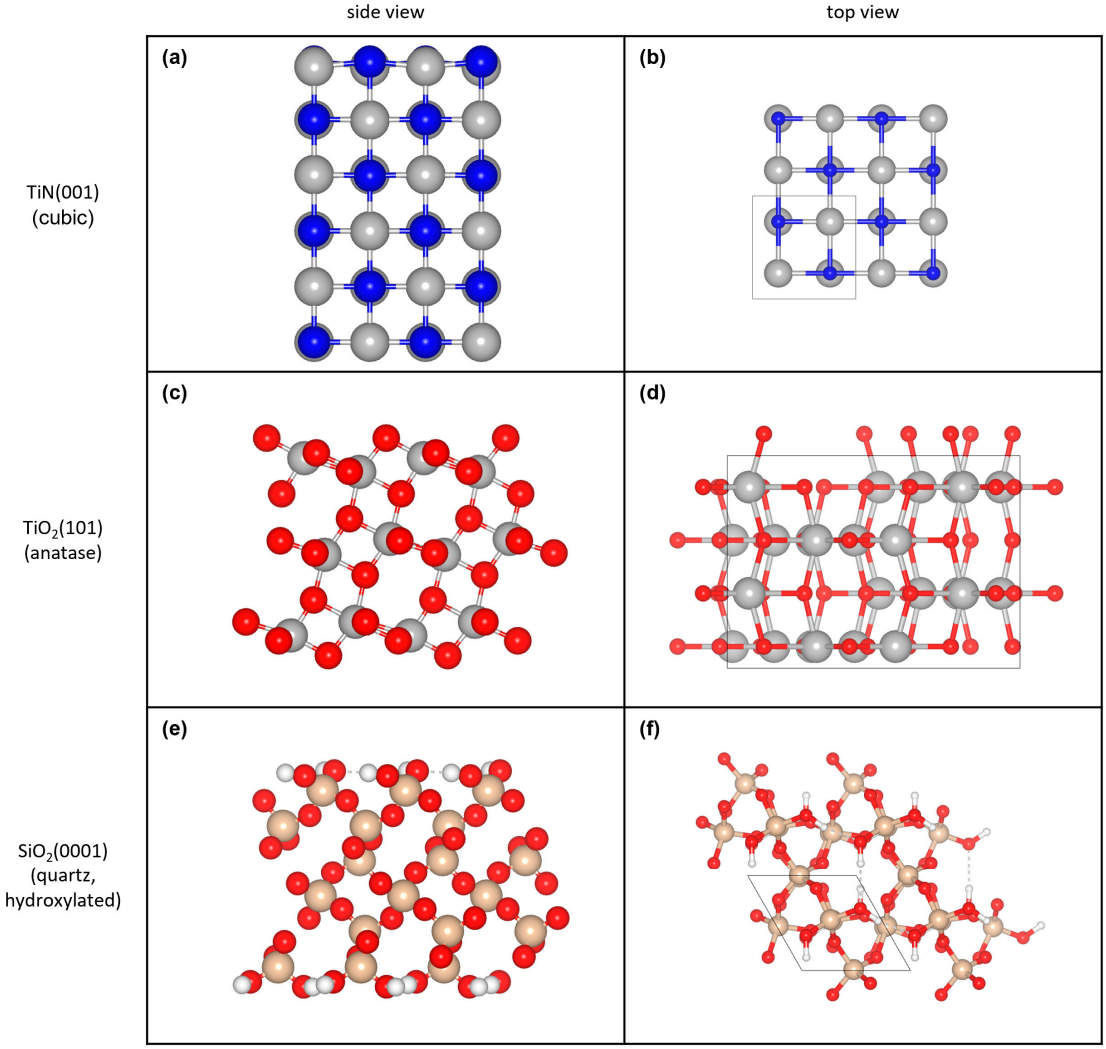

Figure 1. Slab models of cubic TiN(001) (**a**,**b**), anatase TiO_2(101) (**c**,**d**), and quartz SiO_2(0001) (**e**,**f**) surfaces, showing side view (**a**,**c**,**e**) and top view (**b**,**d**,**f**). Ti = gray, Si = brown, O = red, N = blue, and H = white.

Here, $E_{adsorption}$ is the energy of the substrate after adsorption of HF molecules; $E_{byproduct}$ is the sum of the energy of the gaseous byproducts; E_{slab} is the energy of the initial substrate without HF; and E_{HF} is the sum of the energy of HF molecules. For Gibbs free energy (G) calculations, pressure and volume terms are ignored for the solid substrates and only considered for the gaseous molecules, using the following equations.

$$U(T) = U(0) + ZPE + \Delta U(0 \rightarrow T) \quad (2)$$

$$H(T) = U(T) + PV \quad (3)$$

$$G(T) = H(T) - TS = U(0) + ZPE + \Delta U(0 \rightarrow T) + PV - TS \quad (4)$$

$U(0)$, zero-temperature internal energy, can be approximated as electronic energy; ZPE is zero-point vibrational energy; $\Delta U(0 \rightarrow T)$ is internal energy change at finite temperature T; $H(T)$ is enthalpy; and S is entropy. For the calculation of entropy of the surface structures, the rotational and translational degrees of freedom are neglected.

3. Results and Discussions

The chemical reactivity of oxide or nitride surfaces can be strongly affected by the presence and coverage of OH (hydroxyl) or NH (amino) groups on the surfaces [35–41]. At

process-relevant temperatures (ca. 400–600 K) and under vacuum environments, a low OH group density is expected for TiO_2 surfaces [41,42], thus an OH-free bare surface model of TiO_2 is considered. In contrast, SiO_2 surfaces are expected to possess relatively high OH group coverage even at high temperatures and under vacuum [43], and thus were modeled as fully hydroxylated. In the TiN surface case, to the best of our knowledge, there has not been conclusive experimental observation or a thermodynamic model for the coverage of NH or NH_2 groups under fabrication process conditions other than that reporting (100) as the most stable surface orientation [44]. In the kinetic analysis of chemical vapor deposition of TiN, it is often assumed that some NH_2 and NH groups are present on the substrate's surface [45]. Still, it can be suspected that H adatoms on TiN surfaces may easily desorb as H_2, considering the low stability and small diffusion barrier of H adatoms on TiN surfaces [46–48]. In addition, most previous theoretical studies on various surface reactions of TiN assumed bare surface models without terminating functional groups [49–53]. Therefore, a bare TiN(100) surface is assumed as the model for the TiN fluorination.

Figure 2 presents the surface structures of the TiN, TiO_2, and SiO_2 substrates according to the number of HF molecules reacted. Adsorption of HF is assumed to initially occur dissociatively so that F and H adatoms form on the (Ti, Si) and (N, O) atoms of the substrate surfaces, respectively. Then, additional adsorption of HF leads to the formation and desorption of TiF_4 or SiF_4, which creates a vacancy on the surface. It was assumed that the reaction of multiple HF molecules would proceed step-by-step so that the subsequent surface structure from additional HF adsorption originates from the previous reaction's product.

First, when one HF molecule reacts per one Ti atom on the TiN surface, Ti-F(*) and N-H(*) are formed by dissociative HF adsorption, where (*) denotes the surface-adsorbed species. For the adsorption of the second HF per Ti atom, we assumed two F and H form bonds with each surface Ti and N atoms so that Ti-F_2(*) and N-H_2(*) are formed. Afterward, the formation and dissociation of one NH_3 are assumed to occur upon exposure to the third HF per Ti atom, leaving N vacancy and Ti-F_3(*) on the surface. In this structure, some portion of the F atoms is in a bridging configuration between multiple Ti atoms, partially occupying the N vacancy formed by the NH_3 desorption. Thereafter, the formation and dissociation of one TiF_4 occur in the step of reacting four HF molecules per Ti atom, creating another N-H(*) on the surface. The gaseous NH_3 and TiF_4 molecules do not participate in the reaction after being generated as volatile reactants. The considered reactions are summarized in Table 1.

Table 1. The sequential and overall surface reactions of each substate material with HF.

TiN	$TiN(s) + HF(g) \rightarrow TiF(*) + NH(*)$	(reaction 1)
	$TiF(*) + NH(*) + HF(g) \rightarrow TiF_2(*) + NH_2(*)$	(reaction 2)
	$TiF_2(*) + NH_2(*) + HF(g) \rightarrow TiF_3(*) + NH_3(g)$	(reaction 3)
	$TiF_3(*) + HF(g) \rightarrow TiF_4(g) + NH(*)$	(reaction 4)
	Overall : $2TiN(s) + 4HF(g) \rightarrow TiF_4(g) + NH_3(g) + NH(*)$	(reaction 5)
TiO_2	$TiO_2(s) + HF(g) \rightarrow TiF(*) + OH(*)$	(reaction 6)
	$TiF(*) + OH(*) + HF(g) \rightarrow \frac{1}{2}Ti - F(*) + \frac{1}{2}TiF_3(*) + OH(*) + \frac{1}{2}H_2O(g)$	(reaction 7)
	$\frac{1}{2}TiF(*) + OH(*) + HF(g) \rightarrow \frac{1}{2}TiF_3(*) + H_2O(g)$	(reaction 8)
	$TiF_3(*) + HF(g) \rightarrow \frac{1}{2}TiF_4(g) + \frac{1}{2}TiF(*) + \frac{1}{2}H_2O(g)$	(reaction 9)
	Overall : $TiO_2(s) + 4HF(g) \rightarrow \frac{1}{2}TiF_4(g) + \frac{1}{2}TiF(*) + \frac{1}{2}TiF_3(*) + 2H_2O(g)$	(reaction 10)
SiO_2	$SiO_2(s) + 2\,OH(*) + HF(g) \rightarrow SiF(*) + OH(*) + H_2O(g)$	(reaction 11)
	$SiF(*) + OH(*) + HF(g) \rightarrow SiF_2(*) + H_2O(g)$	(reaction 12)
	$SiF_2(*) + HF(g) \rightarrow SiF_3(*) + OH(*)$	(reaction 13)
	$SiF_2(*) + OH(*) + HF(g) \rightarrow SiF_4(g) + 2OH(*)$	(reaction 14)
	Overall : $SiO_2(s) + 4HF(g) \rightarrow SiF_4(g) + 2H_2O(g)$	(reaction 15)

(*) denotes the surface-adsorbed species.

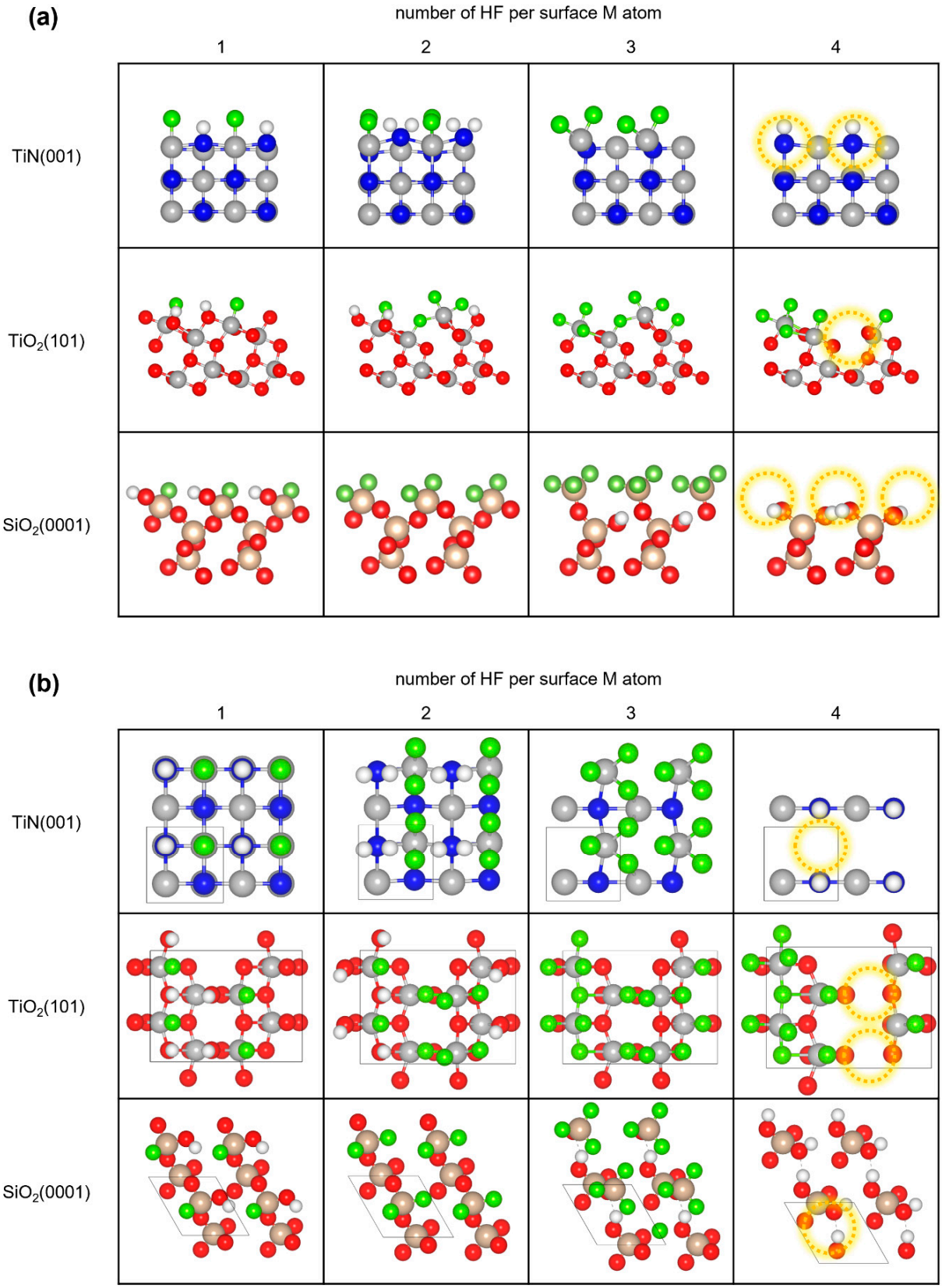

Figure 2. DFT-calculated surface structures of the TiN, TiO_2, and SiO_2 substrates according to the number of HF molecules (1–4) reacted; (**a**) the side view and (**b**) the top view. The removed surface Ti and Si atomic sites are marked with yellow. Ti = gray, Si = brown, F = green, O = red, N = blue, and H = white. A part of the sub-surface atoms is hidden for presentation clarity.

TiO_2 was also considered as a substrate for the HF adsorption and etching of Ti. Because there are four Ti atoms exposed on the TiO_2 surface model, 4, 8, 12, and 16 HF molecules were sequentially considered to react with the TiO_2 substrate. Similar to TiN, Ti-F(*) and O-H(*) are formed by dissociative adsorption of the first HF molecule per Ti atom. Then, the second HF molecule per Ti (8 HF molecules on the calculation cell) is assumed to undergo a disproportionation reaction so that Ti-F(*) and Ti-F_3(*) are formed, and 1/2 H_2O molecule per surface Ti form from the O-H(*) and desorbs at this stage. Here, F atoms bridging between Ti atoms are observable, especially for those in Ti-F_3(*) configurations. After exposure to the third HF per Ti atom (12 HF molecules on the calculation cell), the Ti-F(*) is converted to Ti-F_3(*), leaving one H_2O molecule per Ti. Finally, adsorption of the fourth HF per surface Ti atom would produce TiF_4 and H_2O as gaseous byproducts, leaving Ti and O vacancies and Ti-F(*) and Ti-F_3(*) on the surface. Therefore, we observe the TiO_2 surface becoming rougher at the atomic level upon initial exposure to HF. However, such a locally roughened substrate region can be expected to have a higher chemical etching rate upon further exposure to an additional etchant [54,55], eventually creating a smoother surface.

In the SiO_2 case, the substrate is assumed to be fully hydroxylated, so there are two OH groups per surface Si atom before exposure to HF. Thus, for the first two HF molecules per Si atom, dissociative adsorption of each HF molecule results in the desorption of one H_2O molecule and adsorption of one F on the surface Si atom, first to Si-F(*) and then to Si-F_2(*). Then, the third HF is assumed to break the bond between the surface Si and O, thus a Si-OH is formed below Si-F_3(*). Finally, adsorption of the fourth HF per surface Si atom would produce SiF_4 and H_2O as gaseous byproducts, re-generating two OH groups per now-exposed Si atom.

The reaction energies of TiN, TiO_2, and SiO_2 with HF were calculated and compared (Figure 3a) to compare the tendency toward surface fluorination reactions of various substrates. The energy per HF was calculated by dividing the reaction energy by the number of HFs to compare the reactivity of the three substrates. TiN and SiO_2 substrates reacted with 1, 2, 3, and 4 HF molecules, while TiO_2 reacted with 4, 8, 12, and 16 HF molecules. The calculated energy change values were divided into the respective number of HF molecules, as shown in Figure 3a.

First, in the case of TiN, the adsorption of the first HF into H and F adatoms is exothermic and can be expected to occur. However, because subsequent adsorption of additional HF, resulting in TiF_2(*) and NH_2(*), is highly endothermic (2.0 eV above the initial coverage), it can be predicted that the adsorption of two HF molecules per surface Ti atom would be difficult. Such sudden destabilization by adsorption of additional HF may originate from lateral steric hindrance between the TiF_2(*) and NH_2(*) moieties (Figure 2b). Although the overall energy is stabilized by the adsorption of the third and fourth HF per surface Ti atom to form gaseous NH_3 and TiF_4, respectively, these steps would need to undergo sequential addition of H and F atoms to the N and Ti atoms on the surface. Thus, it can be predicted that the formation of NH_3 and TiF_4 volatile byproducts will be difficult through the fluorination reaction of TiN. Furthermore, the etching of the TiN substrate through fluorination is expected to be difficult to occur.

In contrast, for TiO_2 and SiO_2, each step in the surface reactions with HF is generally exothermic. Furthermore, although some F atoms are suggested to remain after exposure of the computational unit cell to 16 HF molecules, adsorption of more than 16 HF molecules accompanying TiF_4 desorption was found to be continuously exothermic (not shown). Therefore, it is predicted that the chemical etching of TiO_2 and SiO_2 through fluorination by HF is a preferred reaction.

However, it is notable that a fully hydroxylated surface was assumed for SiO_2, allowing for easier H_2O byproduct formation and facilitating the SiF_4 removal; zero OH coverage was assumed on TiO_2. As the etching of SiO_2 by gaseous HF is known to be significantly enhanced by forming a mixture with H_2O [56], similar enhancements may occur for TiO_2 as well. In such a case, the H_2O generated by the HF reaction may further self-catalytically

facilitate the etching reaction of TiO_2. In contrast, the less-than-full actual OH coverage on SiO_2 may result in lower reactivity toward the HF etching in reality.

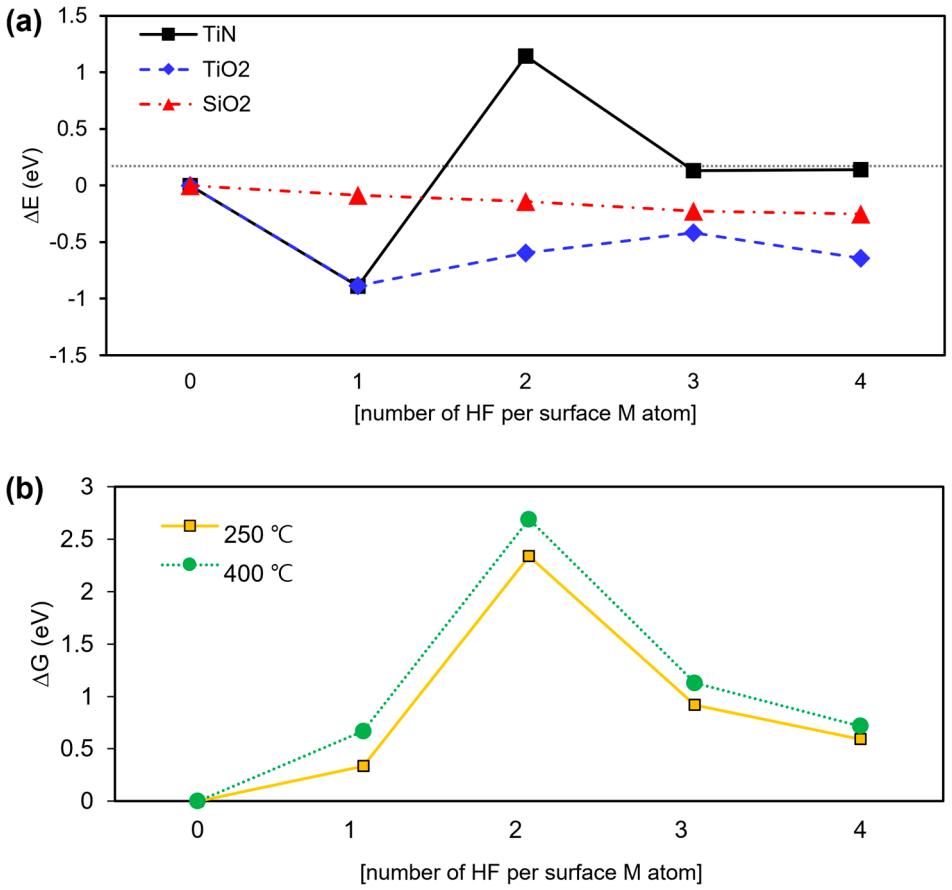

Figure 3. Energy change according to the number of HF molecules adsorbed on the substrates: (**a**) electronic energy of TiN, TiO_2, and SiO_2, and (**b**) Gibbs free energy changes of TiN at 250 °C and 400 °C.

The Gibbs energy difference for each reaction temperature between the substrate and HF was calculated (Figure 3b) to more accurately identify the reaction preference according to temperature. The temperature was compared from 250 to 400 °C, and the partial HF pressure was calculated as 80 mTorr, similar to the conditions in the previous experimental study on TiN ALE [17]. A negative value of the Gibbs free energy change predicts a spontaneous reaction, while a positive value predicts the opposite. The Gibbs free energy change value had a positive value in all reaction steps of TiN and HF. Therefore, it can be predicted that the reaction is nonspontaneous. As the reaction involves the adsorption of multiple gaseous molecules onto a surface of solid material, translation entropy loss of the HF molecules results in nonspontaneous adsorption even for the lowest coverage considered; such an effect is more significant at higher temperatures.

The current observation of preference toward fluorination etching partially agrees with the previous experimental report on the TiN ALE process [17]. For the self-limiting etching conditions to hold so that a constant EPC value can be achieved in such an oxidation-fluorination sequence, the HF pulse should selectively etch only TiO_2 layers on top of the TiN surface but not the bulk of the TiN materials. Therefore, our theoretical observation of selectivity toward initial fluorination showed that HF readily etches TiO_2, but TiN is resistant toward HF adsorption, which explains the core nature of the material properties of TiN versus TiO_2 that govern the ALE process.

The projected density of states (PDOS) of TiN(100) surfaces upon sequential reactions with HF are obtained in order to guide future experimental studies. The PDOS of the bare

TiN(100) surface (Figure 4a) shows good correspondence with the reported properties of the bulk rocksalt TiN in the literature, exhibiting the characteristic metallic nature of which the E_F (Fermi level) is dominated by the Ti atomic orbitals [47,57]. Adsorption of F and H adatoms results in characteristic valence level states, which are F2p at ca. −4 eV and H1s at −7.0 eV below the E_F, respectively (Figure 4b–d). In contrast, the creation of Ti vacancy after removal of TiF4 (Figure 4e) does not significantly alter the PDOS compared to the initial TiN(100) surface.

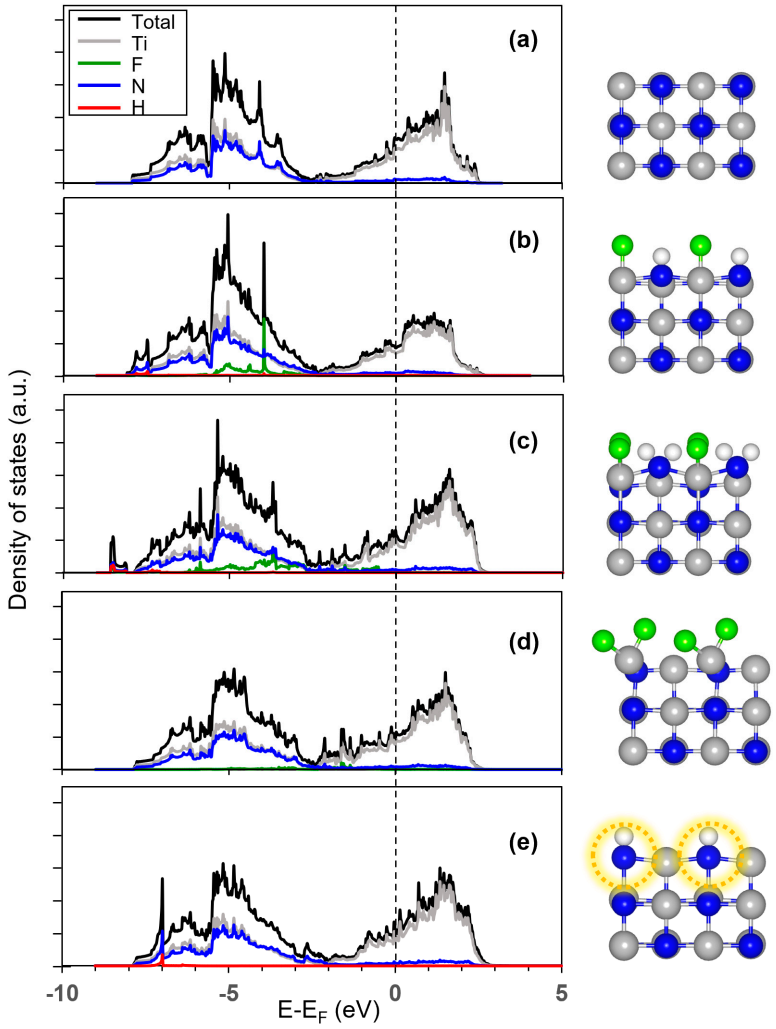

Figure 4. Projected density of states (PDOS) plots of the TiN surface structures upon reaction with HF with varying numbers of HF molecules; (**a**) bare TiN, (**b**–**e**) 1–4 HF per surface Ti, as defined in Figure 2.

4. Conclusions

The fluorination and etching reactions of TiN, TiO_2, and SiO_2 surfaces by HF were investigated using DFT calculations. In the case of TiN, it was confirmed that as the adsorption and etching reactions progressed, the reaction was not favored. It was observed that in the TiO_2 and SiO_2 cases, energy was stabilized as volatile byproducts such as TiF_4, SiF_4, and H_2O were produced. Therefore, it was found that TiO_2 and SiO_2 can be selectively etched by HF, while TiN is resistant to etching in exposure to HF. Therefore, this study clarified the initial surface reaction mechanism of the ALE process on TiN. Future studies on elucidating the surface chemistry of the emerging ALE processes will further help develop unit semiconductor fabrication processes.

Author Contributions: Conceptualization, B.S.; methodology, B.S. and H.O.; software, J.H.J. and H.O.; validation, J.H.J. and H.O.; formal analysis, J.H.J. and H.O.; investigation, J.H.J. and H.O.; resources, B.S.; data curation, J.H.J. and H.O.; writing—original draft preparation, J.H.J.; writing—review and editing, B.S.; visualization, J.H.J.; supervision, B.S.; project administration, B.S.; funding acquisition, B.S. All authors have read and agreed to the published version of the manuscript.

Funding: This research was supported by: Korea Institute for Advancement of Technology (KIAT) grant funded by the Korean Government (MOTIE) (P0012451, The Competency Development Program for Industry Specialist); by the National Research Foundation (NRF) grant funded by the Korean Government (NRF-2021M3H4A6A01048300); and by 2022 Hongik University Research Fund.

Institutional Review Board Statement: Not applicable.

Informed Consent Statement: Not applicable.

Data Availability Statement: Not applicable.

Conflicts of Interest: The authors declare no conflict of interest.

References

1. Kwak, M.Y.; Shin, D.H.; Kang, T.W.; Kim, K.N. Characteristics of TiN Barrier Layer against Cu Diffusion. *Thin Solid Films* **1999**, *339*, 290–293. [CrossRef]
2. Fillot, F.; Morel, T.; Minoret, S.; Matko, I.; Maîtrejean, S.; Guillaumot, B.; Chenevier, B.; Billon, T. Investigations of Titanium Nitride as Metal Gate Material, Elaborated by Metal Organic Atomic Layer Deposition Using TDMAT and NH_3. *Microelectron. Eng.* **2005**, *82*, 248–253. [CrossRef]
3. Lee, C.; Kuo, Y.-L. The Evolution of Diffusion Barriers in Copper Metallization. *JOM* **2007**, *59*, 44–49. [CrossRef]
4. Lima, L.P.B.; Moreira, M.A.; Diniz, J.A.; Doi, I. Titanium Nitride as Promising Gate Electrode for MOS Technology. *Phys. Status Solidi C* **2012**, *9*, 1427–1430. [CrossRef]
5. Lee, B.-J.; Kim, Y.-S.; Seo, D.-W.; Choi, J.-W. The Effect of Deposition Temperature of TiN Thin Film Deposition Using Thermal Atomic Layer Deposition. *Coatings* **2023**, *13*, 104. [CrossRef]
6. Zhang, S.; Zhu, W. TiN Coating of Tool Steels: A Review. *J. Mater. Process. Technol.* **1993**, *39*, 165–177. [CrossRef]
7. Santecchia, E.; Hamouda, A.M.S.; Musharavati, F.; Zalnezhad, E.; Cabibbo, M.; Spigarelli, S. Wear Resistance Investigation of Titanium Nitride-Based Coatings. *Ceram. Int.* **2015**, *41*, 10349–10379. [CrossRef]
8. Datta, S.; Das, M.; Balla, V.K.; Bodhak, S.; Murugesan, V.K. Mechanical, Wear, Corrosion and Biological Properties of Arc Deposited Titanium Nitride Coatings. *Surf. Coat. Technol.* **2018**, *344*, 214–222. [CrossRef]
9. Saha, N.C.; Tompkins, H.G. Titanium Nitride Oxidation Chemistry: An X-ray Photoelectron Spectroscopy Study. *J. Appl. Phys.* **1992**, *72*, 3072–3079. [CrossRef]
10. Kanarik, K.J.; Lill, T.; Hudson, E.A.; Sriraman, S.; Tan, S.; Marks, J.; Vahedi, V.; Gottscho, R.A. Overview of Atomic Layer Etching in the Semiconductor Industry. *J. Vac. Sci. Technol. A* **2015**, *33*, 020802. [CrossRef]
11. Fang, C.; Cao, Y.; Wu, D.; Li, A. Thermal Atomic Layer Etching: Mechanism, Materials and Prospects. *Prog. Nat. Sci. Mater. Int.* **2018**, *28*, 667–675. [CrossRef]
12. Kim, D.S.; Kim, J.E.; Gill, Y.J.; Jang, Y.J.; Kim, Y.E.; Kim, K.N.; Yeom, G.Y.; Kim, D.W. Anisotropic/Isotropic Atomic Layer Etching of Metals. *Appl. Sci. Converg. Technol.* **2020**, *29*, 41–49. [CrossRef]
13. Fischer, A.; Routzahn, A.; George, S.M.; Lill, T. Thermal Atomic Layer Etching: A Review. *J. Vac. Sci. Technol. A* **2021**, *39*, 030801. [CrossRef]
14. Hwang, I.-H.; Cha, H.-Y.; Seo, K.-S. Low-Damage and Self-Limiting (Al)GaN Etching Process through Atomic Layer Etching Using O_2 and BCl_3 Plasma. *Coatings* **2021**, *11*, 268. [CrossRef]
15. Fischer, A.; Mui, D.; Routzahn, A.; Gasvoda, R.; Sims, J.; Lill, T. Surface Reaction Modelling of Thermal Atomic Layer Etching on Blanket Hafnium Oxide and Its Application on High Aspect Ratio Structures. *J. Vac. Sci. Technol. A* **2023**, *41*, 012601. [CrossRef]
16. George, S.M. Mechanisms of Thermal Atomic Layer Etching. *Acc. Chem. Res.* **2020**, *53*, 1151–1160. [CrossRef]
17. Lee, Y.; George, S.M. Thermal Atomic Layer Etching of Titanium Nitride Using Sequential, Self-Limiting Reactions: Oxidation to TiO_2 and Fluorination to Volatile TiF_4. *Chem. Mater.* **2017**, *29*, 8202–8210. [CrossRef]
18. Shinoda, K.; Miyoshi, N.; Kobayashi, H.; Izawa, M.; Ishikawa, K.; Hori, M. Rapid Thermal-Cyclic Atomic-Layer Etching of Titanium Nitride in CHF_3/O_2 Downstream Plasma. *J. Phys. Appl. Phys.* **2019**, *52*, 475106. [CrossRef]
19. Miyoshi, N.; McDowell, N.; Kobayashi, H. Atomic Layer Etching of Titanium Nitride with Surface Modification by Cl Radicals and Rapid Thermal Annealing. *J. Vac. Sci. Technol. A* **2022**, *40*, 032601. [CrossRef]
20. Shim, D.; Kim, J.; Kim, Y.; Chae, H. Plasma Atomic Layer Etching for Titanium Nitride at Low Temperatures. *J. Vac. Sci. Technol. B* **2022**, *40*, 022208. [CrossRef]
21. Miki, N.; Kikuyama, H.; Kawanabe, I.; Miyashita, M.; Ohmi, T. Gas-Phase Selective Etching of Native Oxide. *IEEE Trans. Electron Devices* **1990**, *37*, 107–115. [CrossRef]

22. Kim, D.H.; Kwak, S.J.; Jeong, J.H.; Yoo, S.; Nam, S.K.; Kim, Y.; Lee, W.B. Molecular Dynamics Simulation of Silicon Dioxide Etching by Hydrogen Fluoride Using the Reactive Force Field. *ACS Omega* **2021**, *6*, 16009–16015. [CrossRef] [PubMed]
23. Neyts, E.C.; Brault, P. Molecular Dynamics Simulations for Plasma-Surface Interactions. *Plasma Process. Polym.* **2017**, *14*, 1600145. [CrossRef]
24. Vanraes, P.; Parayil Venugopalan, S.; Bogaerts, A. Multiscale Modeling of Plasma–Surface Interaction—General Picture and a Case Study of Si and SiO_2 Etching by Fluorocarbon-Based Plasmas. *Appl. Phys. Rev.* **2021**, *8*, 041305. [CrossRef]
25. Kondati Natarajan, S.; Elliott, S.D. Modeling the Chemical Mechanism of the Thermal Atomic Layer Etch of Aluminum Oxide: A Density Functional Theory Study of Reactions during HF Exposure. *Chem. Mater.* **2018**, *30*, 5912–5922. [CrossRef]
26. Mullins, R.; Kondati Natarajan, S.; Elliott, S.D.; Nolan, M. Self-Limiting Temperature Window for Thermal Atomic Layer Etching of HfO_2 and ZrO_2 Based on the Atomic-Scale Mechanism. *Chem. Mater.* **2020**, *32*, 3414–3426. [CrossRef]
27. Basher, A.H.; Krstić, M.; Fink, K.; Ito, T.; Karahashi, K.; Wenzel, W.; Hamaguchi, S. Formation and Desorption of Nickel Hexafluoroacetylacetonate $Ni(Hfac)_2$ on a Nickel Oxide Surface in Atomic Layer Etching Processes. *J. Vac. Sci. Technol. A* **2020**, *38*, 052602. [CrossRef]
28. Clancey, J.W.; Cavanagh, A.S.; Smith, J.E.T.; Sharma, S.; George, S.M. Volatile Etch Species Produced during Thermal Al_2O_3 Atomic Layer Etching. *J. Phys. Chem. C* **2020**, *124*, 287–299. [CrossRef]
29. Cheng, E.; Hwang, G.S. Dissociative Chemisorption of Methyl Fluoride and Its Implications for Atomic Layer Etching of Silicon Nitride. *Appl. Surf. Sci.* **2021**, *543*, 148557. [CrossRef]
30. Konh, M.; Janotti, A.; Teplyakov, A. Molecular Mechanism of Thermal Dry Etching of Iron in a Two-Step Atomic Layer Etching Process: Chlorination Followed by Exposure to Acetylacetone. *J. Phys. Chem. C* **2021**, *125*, 7142–7154. [CrossRef]
31. Hu, X.; Schuster, J. Chemical Mechanism of AlF_3 Etching during AlMe3 Exposure: A Thermodynamic and DFT Study. *J. Phys. Chem. C* **2022**, *126*, 7410–7420. [CrossRef]
32. Mullins, R.; Gutiérrez Moreno, J.J.; Nolan, M. Origin of Enhanced Thermal Atomic Layer Etching of Amorphous HfO_2. *J. Vac. Sci. Technol. A* **2022**, *40*, 022604. [CrossRef]
33. Kondati Natarajan, S.; Cano, A.M.; Partridge, J.L.; George, S.M.; Elliott, S.D. Prediction and Validation of the Process Window for Atomic Layer Etching: HF Exposure on TiO_2. *J. Phys. Chem. C* **2021**, *125*, 25589–25599. [CrossRef]
34. Wang, Y.; Zhang, H.; Han, Y.; Liu, P.; Yao, X.; Zhao, H. A Selective Etching Phenomenon on {001} Faceted Anatase Titanium Dioxide Single Crystal Surfaces by Hydrofluoric Acid. *Chem. Commun.* **2011**, *47*, 2829–2831. [CrossRef] [PubMed]
35. Ande, C.K.; Knoops, H.C.M.; de Peuter, K.; van Drunen, M.; Elliott, S.D.; Kessels, W.M.M. Role of Surface Termination in Atomic Layer Deposition of Silicon Nitride. *J. Phys. Chem. Lett.* **2015**, *6*, 3610–3614. [CrossRef] [PubMed]
36. Yusup, L.L.; Park, J.-M.; Noh, Y.-H.; Kim, S.-J.; Lee, W.-J.; Park, S.; Kwon, Y.-K. Reactivity of Different Surface Sites with Silicon Chlorides during Atomic Layer Deposition of Silicon Nitride. *RSC Adv.* **2016**, *6*, 68515–68524. [CrossRef]
37. Choi, W.; Lee, S.; Han, D.-H.; Lim, H.T.; Park, H.; Lee, G.-D. Reaction Mechanisms of Chlorine Reduction on Hydroxylated Alumina in Titanium Nitride Growth: First Principles Study. *Appl. Surf. Sci.* **2021**, *550*, 149391. [CrossRef]
38. Kim, H.-M.; Lee, J.-H.; Lee, S.-H.; Harada, R.; Shigetomi, T.; Lee, S.; Tsugawa, T.; Shong, B.; Park, J.-S. Area-Selective Atomic Layer Deposition of Ruthenium Using a Novel Ru Precursor and H_2O as a Reactant. *Chem. Mater.* **2021**, *33*, 4353–4361. [CrossRef]
39. Lee, J.; Lee, J.-M.; Oh, H.; Kim, C.; Kim, J.; Kim, D.H.; Shong, B.; Park, T.J.; Kim, W.-H. Inherently Area-Selective Atomic Layer Deposition of SiO_2 Thin Films to Confer Oxide Versus Nitride Selectivity. *Adv. Funct. Mater.* **2021**, *31*, 2102556. [CrossRef]
40. Ta, H.T.T.; Bui, H.V.; Nguyen, V.-H.; Tieu, A.K. Reactions between $SiCl_4$ and H_2O on Rutile TiO_2 Surfaces in Atomic Layer Deposition of SiO_2 by First-Principles Calculations. *Surf. Interfaces* **2023**, *36*, 102454. [CrossRef]
41. Kamphaus, E.P.; Shan, N.; Jones, J.C.; Martinson, A.B.F.; Cheng, L. Selective Hydration of Rutile TiO_2 as a Strategy for Site-Selective Atomic Layer Deposition. *ACS Appl. Mater. Interfaces* **2022**, *14*, 21585–21595. [CrossRef] [PubMed]
42. Walle, L.E.; Borg, A.; Johansson, E.M.J.; Plogmaker, S.; Rensmo, H.; Uvdal, P.; Sandell, A. Mixed Dissociative and Molecular Water Adsorption on Anatase TiO_2(101). *J. Phys. Chem. C* **2011**, *115*, 9545–9550. [CrossRef]
43. Zhuravlev, L.T. The Surface Chemistry of Amorphous Silica. Zhuravlev Model. *Colloids Surf. Physicochem. Eng. Asp.* **2000**, *173*, 1–38. [CrossRef]
44. Wang, C.; Dai, Y.; Gao, H.; Ruan, X.; Wang, J.; Sun, B. Surface Properties of Titanium Nitride: A First-Principles Study. *Solid State Commun.* **2010**, *150*, 1370–1374. [CrossRef]
45. Imhoff, L.; Bouteville, A.; Remy, J.C. Kinetics of the Formation of Titanium Nitride Layers by Rapid Thermal Low Pressure Chemical Vapor Deposition from $TiCl_4$-NH_3-H_2. *J. Electrochem. Soc.* **1998**, *145*, 1672. [CrossRef]
46. You, M.S.; Nakanishi, N.; Kato, E. The Equilibrium of the Chemisorption of $TiCl_4$, H_2, and N_2 on Titanium Nitride. *J. Electrochem. Soc.* **1991**, *138*, 1394. [CrossRef]
47. Marlo, M.; Milman, V. Density-Functional Study of Bulk and Surface Properties of Titanium Nitride Using Different Exchange-Correlation Functionals. *Phys. Rev. B* **2000**, *62*, 2899–2907. [CrossRef]
48. Siodmiak, M.; Govind, N.; Andzelm, J.; Tanpipat, N.; Frenking, G.; Korkin, A. Theoretical Study of Hydrogen Adsorption and Diffusion on TiN(100) Surface. *Phys. Status Solidi B* **2001**, *226*, 29–36. [CrossRef]
49. Phung, Q.M.; Vancoillie, S.; Pourtois, G.; Swerts, J.; Pierloot, K.; Delabie, A. Atomic Layer Deposition of Ruthenium on a Titanium Nitride Surface: A Density Functional Theory Study. *J. Phys. Chem. C* **2013**, *117*, 19442–19453. [CrossRef]
50. Seifitokaldani, A.; Savadogo, O.; Perrier, M. Density Functional Theory (DFT) Computation of the Oxygen Reduction Reaction (ORR) on Titanium Nitride (TiN) Surface. *Electrochim. Acta* **2014**, *141*, 25–32. [CrossRef]

51. Kura, C.; Kunisada, Y.; Tsuji, E.; Zhu, C.; Habazaki, H.; Nagata, S.; Müller, M.P.; De Souza, R.A.; Aoki, Y. Hydrogen Separation by Nanocrystalline Titanium Nitride Membranes with High Hydride Ion Conductivity. *Nat. Energy* **2017**, *2*, 786–794. [CrossRef]
52. Wang, Y.; Fu, Z.; Zhang, X.; Yang, Z. Understanding the Correlation between the Electronic Structure and Catalytic Behavior of TiC(001) and TiN(001) Surfaces: DFT Study. *Appl. Surf. Sci.* **2019**, *494*, 57–62. [CrossRef]
53. Sharma, V.; Kondati Natarajan, S.; Elliott, S.D.; Blomberg, T.; Haukka, S.; Givens, M.E.; Tuominen, M.; Ritala, M. Combining Experimental and DFT Investigation of the Mechanism Involved in Thermal Etching of Titanium Nitride Using Alternate Exposures of NbF_5 and CCl_4, or CCl_4 Only. *Adv. Mater. Interfaces* **2021**, *8*, 2101085. [CrossRef]
54. Fang, Z.; Zhang, Y.; Li, R.; Liang, Y.; Deng, H. An Efficient Approach for Atomic-Scale Polishing of Single-Crystal Silicon via Plasma-Based Atom-Selective Etching. *Int. J. Mach. Tools Manuf.* **2020**, *159*, 103649. [CrossRef]
55. Gerritsen, S.H.; Chittock, N.J.; Vandalon, V.; Verheijen, M.A.; Knoops, H.C.M.; Kessels, W.M.M.; Mackus, A.J.M. Surface Smoothing by Atomic Layer Deposition and Etching for the Fabrication of Nanodevices. *ACS Appl. Nano Mater.* **2022**, *5*, 18116–18126. [CrossRef]
56. Helms, C.R.; Deal, B.E. Mechanisms of the HF/H_2O Vapor Phase Etching of SiO_2. *J. Vac. Sci. Technol. A* **1992**, *10*, 806–811. [CrossRef]
57. Yu, S.; Zeng, Q.; Oganov, A.R.; Frapper, G.; Zhang, L. Phase Stability, Chemical Bonding and Mechanical Properties of Titanium Nitrides: A First-Principles Study. *Phys. Chem. Chem. Phys.* **2015**, *17*, 11763–11769. [CrossRef]